X-ray focusing using lobster-eye optics: a comparison of theory with experiment.

A.G.Peele and K.A.Nugent
School of Physics
The University of Melbourne
Parkville, Vic., 3052, Australia

A.V.Rode
Laser Physics Centre
Research School of Physical Sciences & Engineering
Australian National University
GPO Box 4
Canberra City, ACT, 2601 Australia

K.Gabel & M.C.Richardson
Centre for Research and Education in Optics and Lasers
University of Central Florida
Orlando, Florida, 32826, USA

R.Strack & W.Siegmund
Schott Fiber Optics Inc
122 Charlton Street
Southbridge, Massachusetts, 01550-1960, USA

ABSTRACT

We report investigations of the x-ray focusing of a square channel capillary array. We use x-rays with an energy of about 1.5 keV from a laser produced plasma. We find the focal structure to be consistent with theoretical expectations. The images were recorded using x-ray film and, to within the precision with which we were able to analyse the results, the data is consistent with an array with negligible channel tilt and a surface roughness of 1.5 nm rms. This is the best performance yet reported for lobster-eye x-ray optics.

Keywords: x-rays, x-ray focusing, lobster-eye optics, microchannel plates

1. INTRODUCTION

X-ray optics based on either single or multiple capillaries have received considerable interest over the past few years. Single capillary optics have been developed for micro-analysis and micro-fluorescence studies using synchrotron and laboratory x-ray sources[1] and multiple capillaries arrays such as the Kumakhov lens[2] and microchannel plate optics[3] have been developed for applications to medicine, lithography and a range of other areas.

Workers in x-ray astronomy[4,5] have taken a particular interest in the development of the microchannel plate device as, when curved into a spherical geometry and using square profile channels, it becomes equivalent to the so-called lobster-eye telescope first proposed by Angel[6] and is closely related to the orthogonal mirror proposal of Schmidt[7]. Chapman *et. al.*[8] have published an exhaustive theoretical treatment of the properties of square channel arrays.

0-8194-1874-9/95/$6.00

The cruciform structure of the focal spot for square profile channels was observed in the x-ray region for the first time by Fraser *et. al.*[9] though the focal spot was itself somewhat broader than was expected due to imperfections in the array. In this paper we report cruciform focal structures that are very close to the theoretical predictions although the overall efficiency is somewhat diminished due to the effects of surface roughness and channel defects. However, with these effects incorporated into the model, excellent agreement was found between theory and experiment. Accordingly, the micro-channel array is rapidly evolving towards becoming a useful and practical x-ray optical device.

2. PRINCIPLE OF OPERATION

The principal of the lobster-eye lens is based on the visual system of macruran crustaceans (lobsters, shrimps and crayfish)[10] and has been discussed a number of times in other publications[3-6]. The central idea is illustrated in figure 1 where, for a one-dimensional lens, an array of mirrors will bring a distant source of x-rays to a focus. In two dimensions, the x-rays need to be reflected from a surface perpendicular to that shown in figure 1 and so an array of square channels will bring the radiation to a focus in two dimensions. In the case that the array is bent to a spherical surface the optic has no preferred axis and so is able to focus equally well in all directions. It is this property which makes the lobster eye a candidate for a wide field of view telescope.

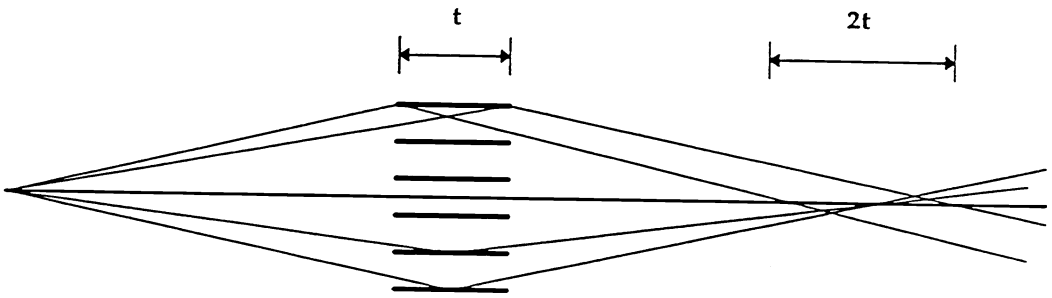

Figure 1: Principle of one dimensional focusing. Note focal aberration due to channel length.

The focusing performance of the lobster-eye lens may be effectively understood using the theoretical results published by Chapman *et. al.*[8]. The lobster-eye lens consists of an array of square channels. Those x-rays that strike the walls of the channels are lost. Of those that enter a channel a fraction that reflects once off two orthogonal walls is reflected into the focal spot, another fraction is reflected only from one wall and so is focused in one dimension to a line passing through the two dimensional focus, and a third fraction passes straight through the array to form an unfocused background. Higher order reflections are also possible but the x-ray photons from such reflections strike a detector as if they were in one of the above classes. The resulting focal structure then consists of a bright focused spot with a fainter cross centred on this and an much less intense diffuse background. The relative numbers of photons in each of the above structures depends on the ratio of the length of a channels to its length and, at the optimum ratio for a lens with no axis of symmetry. As a rough rule of thumb, about 25% of the photons are focused into the central square, 25% end up in each of the one dimensional foci (arms) and 25% end up in the unfocused background. The focusing efficiency in a given direction may be improved by imposing a preferred axis on the device[8] but this is not consistent with a very wide field of view telescope.

The x-rays are brought to a focus with an angular resolution comparable to the angle that an individual channel subtends at the detector. In practise, this implies that the lobster-eye telescope will always be limited in resolution by the physical size of the individual channels. This also leads us to the conclusion that the lobster-eye's promise is primarily as an all-sky x-ray monitor. As a true focusing device, the lobster-eye will be able to image objects very effectively against the diffuse sky background and so may allow the observation of the time history of objects that are currently undetectable.

3. EXPERIMENTAL ARRANGEMENT

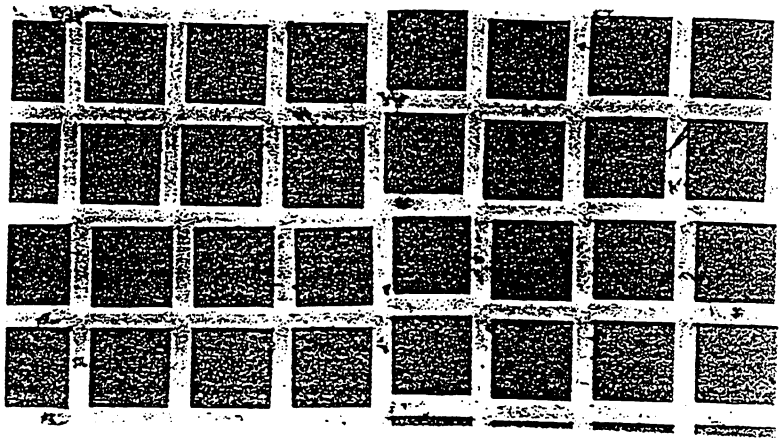

Figure 2: Micrograph of a Schott MCP.

The square channel arrays used in our experiment were microchannel plates (MCP's) manufactured by Schott Fiber Optics, using a proprietary technique which ensured channels exhibit a high degree of squareness and which reduces etching time thereby, in principle, reducing surface roughness in the etched channels. The general procedure for manufacture of MCP's has been discussed elsewhere[11]. A micrograph of the MCP used is shown in figure 2.

The x-rays were generated using a laser-produced plasma created by a 17 nS, 17 J pulse of laser radiation (λ = 1.064 nm) was focussed through an F/10 lens onto a copper target inside an evacuated chamber.

Plasma line and continuum radiation around 1.5 keV was produced as well UV and visible light and debris ejected from the source. Images were recorded on Kodak DEF x-ray film. The film was developed and fixed using the procedure given by Henke *et. al.*[12]. To measure intensity a Joyce-Lobels densitometer with matched N.A. = 0.1 optics was used to record the optical density of the film. The results given by Henke *et. al.*[12] were then used to calculate the intensity. Aluminium foil was used as a filter to protect the x-ray film from visible light and debris. The angle of the target to the film and screening by the MCP also protected the film from debris.

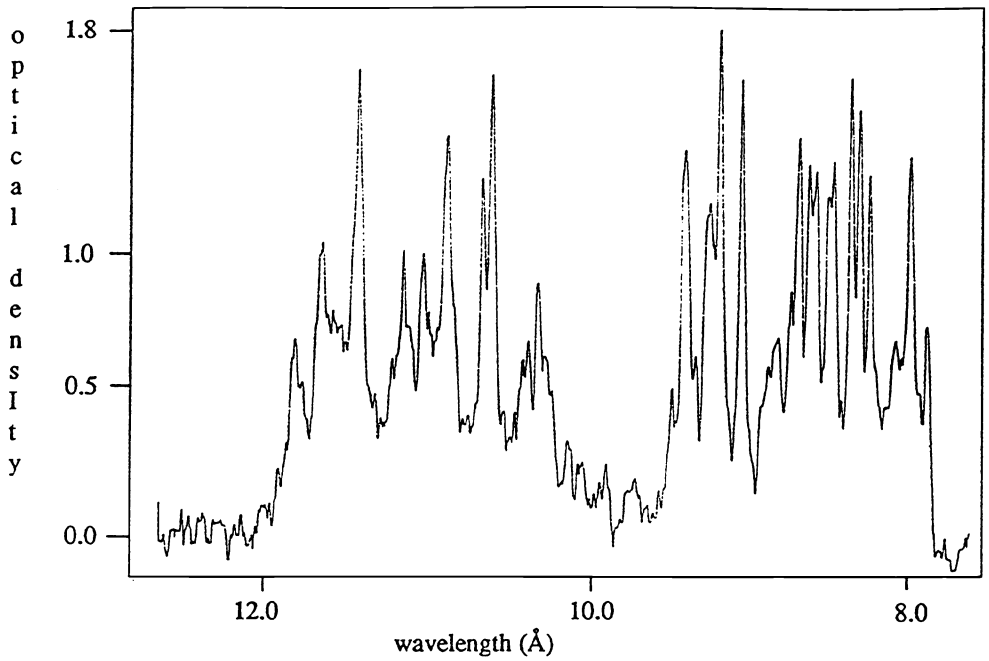

Figure 3: Spectra of the plasma recorded on Kodak DEF film using a flat RAP crystal.

Figure 3 shows the spectrum measured from the plasma using a flat RAP crystal. The crystal interplanar spacing is 26.116 Å and the spectrum from 15° to 30° was measured. A filter of 10 μm Al was used in recording the spectrum. During the actual experiment the filter was 60 μm thick Al. When the optical density is converted to intensity and the effect of transmission through an additional 50 μm of Al is taken into account, it is clear that more than 90% of the radiation reaching the film is between 1.36 keV and 1.56 keV, the absorption edge of Al. In analysing the data we made the simplifying assumption that the x-ray energy was monochromatic and was an energy of 1.5 keV.

Each plate we investigated was 1.5 cm square, channel side length was 200 μm and channel length was 6 mm. Wall thickness was 40 μm. The MCP's were mounted on a 2-axis adjustable stage with a source-MCP and MCP-film distance of 237 mm. The source, MCP and film were all inside an evacuated chamber.

4. RESULTS

Figure 4 shows a 2 dimensional optical density map taken using a scanning densitometer. The optical density recorded with this instrument is diffuse density. Therefore the optical density recorded at any point is affected by the distribution of density about it. It is possible to convert between specular and diffuse optical density[12] however, with an image such as that recorded here, the problem is compounded by the need to deconvolve the effect of the structure in the image. Accordingly, we have used only directly measured specular densities for calculations involving the intensity of the x-rays. However, the two dimensional image still provides us with useful information about the structure of the image. The checkerboard pattern due to shading by channel walls in the MCP can be clearly seen, even along the focal arms. The expected focal distribution is also observed. While there is some flaring along the focal arms, the effect is relatively small. This indicates that the MCP is extremely well produced. Some channel irregularities can also be observed.

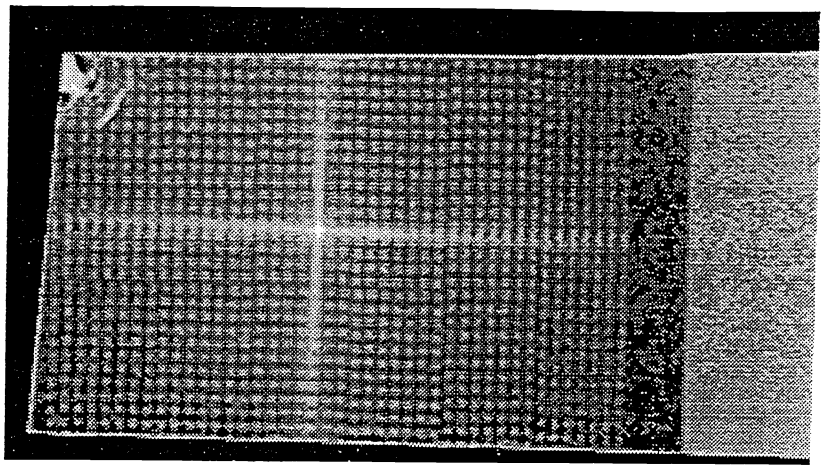

Figure 4: Scanning densitometer recording of focal plane.

Figure 5 shows a one dimensional intensity trace taken along one of the focal arms. The full width at half maximum (FWHM) of the central focus is 230 μm compared to 200 μm expected for a geometrically perfect MCP. The angular resolution is therefore very close to that for a perfect MCP which is fixed by the channel size and object distance alone. In this case, angular resolution is 3.3 arc minutes compared to 2.9 arc minutes for a perfect MCP.

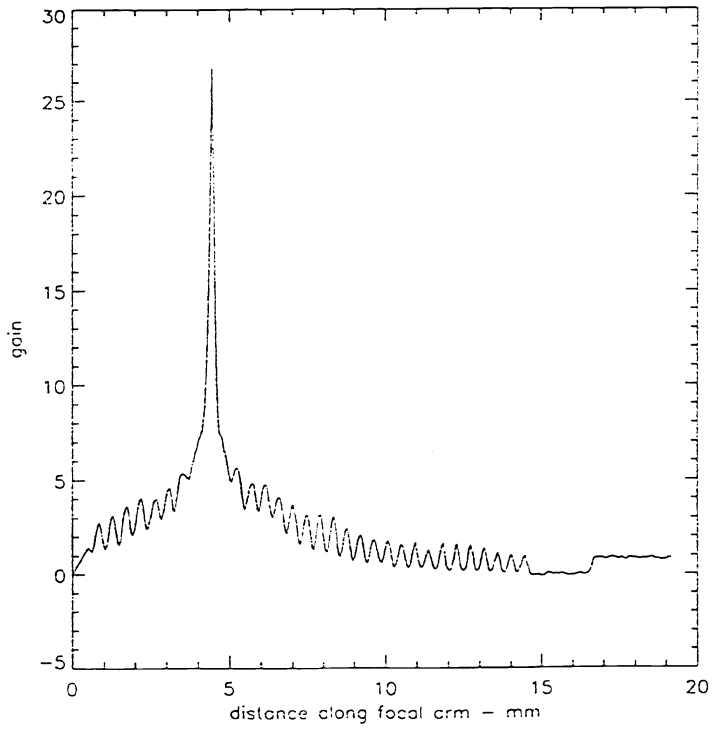

Figure 5: One dimensional scan, along a focal arm, of intensity gain.

A second prime indicator of the quality of an MCP is the efficiency with which the radiation is brought to the focus. A section of the film was exposed directly to the source, enabling us to estimate the intensity of the unfocused flux. We define the ratio of the intensity of the focused flux to the intensity of the unfocused flux as the gain. The gain figure thus calculated can be compared to the theoretical gain which would be obtained for a geometrically perfect and perfectly smooth MCP. We compare both peak gain and average gain over the FWHM. Peak gain is the peak gain recorded in a collection area equal to the slit size of the densitometer used to record the optical density; in our case 100 μm. The average gain over the FWHM is the average gain for a one dimensional scan along one of the focal arms using the same collector size as that used in the peak measurement.

We measure the peak gain in the central focus to be 27 ± 4, while the average gain over the FWHM of the focal region is 21 ± 2. The expected peak gain was calculated by a Monte Carlo ray tracing simulation, for a perfect MCP for the experimental parameters, and was found to be 83. The average gain over the FWHM for a perfect MCP was 62.

Obvious departures from the simulated intensity distribution are reduction and broadening of the central peak and the diminution in intensity along the focal arms. These departures can be explained by a simple model of surface roughness, channel rotation and channel tilt.

Surface roughness reduces the intensity in the reflected beam, and hence in the focus. Flux is also scattered away from the direction of the specular beam due to surface roughness13. We use the Debye-Waller factor14 with σ equal to the rms roughness to calculate the reduction in intensity in the specularly reflected beam. For the purpose of this model we take no account of diffusely scattered x-rays, simply treating such rays as lost.

Rotation of a channel by a certain amount has the effect of rotating the flux distribution from that channel by an equal amount. Consequently, the focal square will tend to become circular and the focal arms will flare out. The effect in measured intensity is therefore greatest in the focal arms, causing intensity to drop off dramatically along the arms. In the focal square this effect tends to cause the focal square to become circular. We characterise rotations as randomly occurring with an rms rotation equal to ϕ. For the purpose of this model we take no account of the fact that, on observation, channel rotations appear to be correlated with fibre bundles within the MCP.

Channel tilt causes the reflected ray to deviate by twice the tilt. This will appear as blur in the image. The central focus will be particularly affected as there are two reflections for centrally focused rays. We characterise tilts along the optic axis as randomly occurring with an rms tilt equal to ξ.

We incorporated these parameters into our ray tracing simulation and found best agreement with our data with the parameters: σ=1.5 nm rms; ϕ=45 mrad rms; and ξ=0.05 mrad rms.

AFM and the sample should also be noted. To obtain accurate results, the structure in the roughness over various length scales and the effects of diffuse scattering will probably be required.

As for other MCP's which have been investigated[15], we observe rotations within a fibre bundle and between adjacent fibre bundles. In our case, ~17 mrad and ~20 mrad respectively. Over several fibre bundles the net misalignment may therefore be of the order of the 45 mrad used in the simulation. Again, it is likely that for accurate comparison, a more detailed model should be used. In this case, the distribution of rotations including the correlation of rotation with fibre bundles, should be included.

We have not attempted any direct measurement of channel tilts. However, channel tilt appears to be negligible from the simulation.

6. CONCLUSION

We have demonstrated x-ray focusing with resolution very close to the theoretical ideal. This promises well for the prospects of realising Angel's lobster eye telescope, if similar performance can be translated into a spherical geometry. We have also demonstrated the ability to model observed results in terms of a simplified model of surface roughness, channel rotations and channel tilts. This model gives us qualitative agreement with direct measurements of those parameters and, to first order, should serve as a useful predictive tool for the performance of future MCP's.

7. ACKNOWLEDGMENTS

We acknowledge the support of a research grant from the Australian Research Council. AGP acknowledges the support of a Commonwealth Postgraduate research award.

8. REFERENCES

1 E.A.Stern, Z.Kalman, A.Lewis and K.Lieberman, *Simple method for focusing x-rays using tapered capillaries*, Appl.Opt., **27**, 5135-5139 (1988)

2 M.A.Kumakhov and F.F.Komarov, *Multiple reflection from surface x-ray optics*, Phs.Reports, **191**, 289-350 (1990)

3 S.W.Wilkins, A.Stevenson, K.Nugent, H.N.Chapman and S.Steenstrup, *On the concentration, focusing and collimation of x-rays and neutrons using microchannel plates and configurations of holes*, Rev.Sci.Instrum., **60**, 1026-1036 (1989)

4 G.W.Fraser, J.E.Lees, J.F.Pearson, M.R.Sims and K.Roxburgh, *X-ray focusing using microchannel plates*, in Multilayer and Grazing Incidence X-Ray/EUV Optics, R.B.Hoover editor, Proc. SPIE, **1546**, 41-52 (1992)

5 P.Kaaret, P.Geissbuhler, A.Chen and E.Glavinas, *X-ray focusing using microchannel plates*, Appl. Opt., **31**, 7339-7343 (1992)

6 J.R.PAngel, *The Lobster-eye Telescope*, Astrophys.J., **233**, 364-373 (1979)

7 W.K.H.Schmidt, *A proposed x-ray focusing device with wide field of view for use in x-ray astronomy*, Nucl.Instrum.Meth., **127**, 285-292 (1975)

8 H.N.Chapman, K.A.Nugent and S.W.Wilkins, *X-ray focusing using square channel capillary arrays*, Rev.Sci.Instrum., **62**, 1542-1561 (1991)

9 G.W.Fraser, A.N.Brunton, J.E.Lees, J.F.Pearson and W.B.Feller, *X-ray focusing using square-pore microchannel plates: First observation of cruxiform image structure*, Nucl.Instrum.Meth., **A324**, 404-407 (1993)

10 See, for example, M.F.Land, *Animal eyes with mirror optics*, Scientific American, **239**, 88-99 (1978)

11 See, for example, H.N.Chapman, *X-ray optics using capillary arrays*, Ph.D. Thesis, University of Melbourne (1992)

12 B.L.Henke, J.Y.Uejio, G.F.Stone, C.H.Dittmore and F.G.Fujiwara, *High-energy x-ray response of photographic films: models and measurement*, J.Opt.Soc.Am., **B3**, 1540-1550 (1986)

13 Y.Yoneda, *Anomalous surface reflection of x rays*, Phys.Rev., **131**, 2010-2013 (1963)

14 P.Debye, *Interference of Röntgen rays and heat motions*, Ann.Phys., **43**, 49-95

15 G.W.Fraser, A.N.Brunton, J.E.Lees, J.F.Pearson, R.Willingale, D.L.Emberson, W.B.Feller, M.Stedman, and J.Haycocks, *Development of microchannel plate (MCP) x-ray optics*, in Multilayer and Grazing Incidence X-Ray/EUV Optics III, R.B.Hoover and A.B.C.Walker Jr., editors, Proc.SPIE., **2011**, (1993)